

# Study on Imaging with Current Excitation Conductivity Imaging Object Based on Magneto-acoustic Effect

Zhang Shun-qi, Yin Tao, Ma Ren, Liu Zhi-peng\*, Member, IEEE

(Institute of Biomedical Engineering, Chinese Academy of Medical Sciences & Peking Union Medical College, Tianjin 300192, China)

**Abstract**—Magneto-acoustic imaging with electrical excitation is a newly proposed approach to image electrical conductivity of biological tissue non-invasively. In this paper, the imaging method is studied using computer simulations and experiments. In this way, a static magnetic field and a microsecond sine pulse stimulations were imposed on the objects such as a copper coil or a agar phantom. The acoustic responses generated by magneto-acoustic effect were detected and analyzed. The finite element method was applied in magneto-acoustic simulation, while an experimental setup was established to measure the acoustic signal from the conductivity imaging objects. The conductivity boundary image was reconstructed from the measured data. Simulation results showed that the distribution of the acoustic source could reflect the sharp change of conductivity produced by the boundary of the objects. Results of the simulation and experiment were in a good agreement, and the resolution of the reconstructed images was less than 1 cm. Our investigation proves the feasibility of the electrical excitation magneto-acoustic imaging method to reflect the conductivity information, providing a foundation of further study on tissues with complex conductivity distribution.

## I. INTRODUCTION

Bioelectrical properties reflect the physical and pathological changes of tissue [1]. Early studies showed that [2]-[5], the conductivity of the cancerous tissue is 6.4 times, while the permittivity is 3.8 times, as the normal tissue. Therefore, early diagnosis using bioimpedance imaging is crucial to the patient to receive early treatment and to prolong the lifespan.

Magneto-acoustic tomography (MAT) [6] is a newly proposed functional imaging approach to noninvasive electrical conductivity imaging of biological tissue. This method converts the electromagnetic excitation to sonic response, which avoid the current disperse effect of electrical impedance tomography (EIT). So it can reach the high resolution of ultrasonic imaging and the high conductivity contrast of EIT. These advantages make it valuable to the tumor diagnosis research with early stages [9][10].

We will investigate the imaging method of MAT with current excitation in this paper. Simulations and experiments

\*Research supported by National Natural Science Foundation of China (81171424) (51137004).

Zhang Shun-qi is with the Institute of Biomedical Engineering, CAMC&PUMC; 7#,Baidi Road, Nankai District, Tianjin, 300192, China.

Yin Tao is with the Institute of Biomedical Engineering, CAMC&PUMC, Tianjin, 300192, China;

Corresponding author: Liu Zhi-peng is with the Institute of Biomedical Engineering, CAMC&PUMC, China; email: lzpeng67@163.com

of the metal coil and agar phantom will be conducted and discussed. The corresponding results will be given.

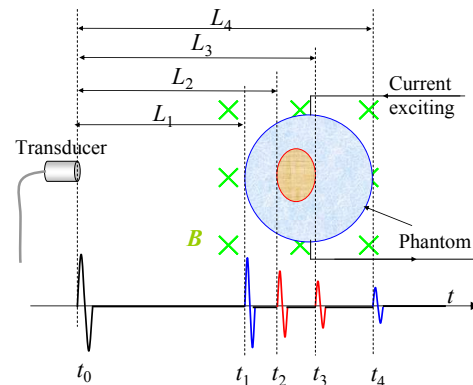
## II. THEORY

In MAT imaging method, the object is placed in a static magnetic field. A time-varying current excitation with several  $\mu$ s pulse width is imposed to the object. Consequently, the combination of the excitation current and the static magnetic field will make the object affected by Lorentz force. Thus, an ultrasonic wave will be produced. As Fig. 1 shows, suppose the inner and outer layer of the phantom has different conductivities. The distances between the transducer and the conductivity boundaries are  $L_1, L_2, L_3,$  and  $L_4$  respectively. The transmission time intervals are  $t_1-t_0, t_2-t_0, t_3-t_0, t_4-t_0$ . Suppose the phantom is an acoustically homogenous medium, the acoustic velocity is  $v_s$ , if the delay of the transducer is ignored, we get —

$$\frac{L_1}{t_1 - t_0} = \frac{L_2}{t_2 - t_0} = \frac{L_3}{t_3 - t_0} = \frac{L_4}{t_4 - t_0} = v_s \quad (1)$$

It demonstrates that the measured acoustic signal reflects the boundary distribution of the medium. Thus, the ultrasonic waves are collected by the transducers located around the object for image reconstruction.

Figure 1 Theory of the magneto-acoustic imaging with electrical excitation



The ultrasonic wave pressure is a function of current density and the magnetic field.

According to the electromagnetics, the medium is affected by the Lorentz force

$$d\mathbf{F} = \mathbf{I}d\mathbf{l} \times \mathbf{B} \quad (2)$$

Where  $\mathbf{I}$  is the uniform vector of length,  $\mathbf{B}$  is flux density of the static magnetic field,  $\mathbf{F}$  is Lorentz force,  $\mathbf{I}$  is excitation current in the object.

Use the Ohm's law, we get

$$I = U / R \quad (3)$$

Where  $U$  is the voltage excitation,  $R$  is the equivalent resistance of the medium. So the current in the medium is relevant to the voltage excitation and the conductivity of the medium [13].

According the law of conservation of mass [6],

$$\frac{\partial(\rho_0 + \rho)}{\partial t} = -\nabla \cdot (\rho_0 \mathbf{v} + \rho \mathbf{v}) \quad (4)$$

Where  $t$  is time,  $\rho_0$  is medium density,  $\rho$  is the change of the medium density,  $\mathbf{v}$  is velocity of the mass point.

Euler's equation [6],

$$(\rho_0 + \rho) \left( \frac{\partial \mathbf{v}}{\partial t} + \mathbf{v} \cdot \nabla \mathbf{v} \right) + \nabla (p_0 + p) - \mathbf{J} \times \mathbf{B} = 0 \quad (5)$$

Where  $\mathbf{J}$  is current density,  $p$  is acoustic pressure,  $p_0$  is acoustic pressure change.

The relation between instantaneous density and acoustic pressure is [6],

$$p = c_s^2 \rho \quad (6)$$

Where  $c_s = \sqrt{1 / \rho_0 \beta_s}$ ,  $\beta_s$  is the adiabatic compressibility of the medium.

Using the equations above, we can deduce the wave equation as [1]

$$\nabla^2 p - \frac{1}{c_s^2} \frac{\partial^2 p}{\partial t^2} = \nabla \cdot (\mathbf{J} \times \mathbf{B}) \quad (7)$$

After using Green's function, the solution of (7) can be solved as [1]

$$p(\mathbf{r}, t) = \frac{-1}{4\pi R} \int d\mathbf{r}' \nabla_{r'} \cdot [\mathbf{J}(\mathbf{r}') \times \mathbf{B}(\mathbf{r}')] \frac{\delta(t - \frac{R}{c_s}}{R} \quad (8)$$

Where  $\mathbf{R} = |\mathbf{r} - \mathbf{r}'|$  and the integration is over the sample volume.

Then, the electrical distribution can be reconstructed by using back-projection arithmetic from measured signal detected by the transducer. Finally, the conductivity image of the object can be obtained.

## I. METHODS

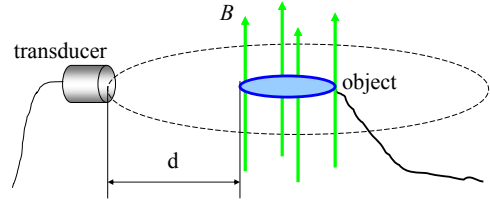
### A. Simulation method

The simulation scheme is showed in Fig. 2. In order to study the MAT imaging method, meanwhile to make the sonic response easy to be received, we chose the copper coil as the imaging object in MAT simulation and experiment study. The coil is placed in a static magnetic field, which the flux density  $B$  is 0.4T.

Considering the voltage is ratio to the current according to the Ohm's Law(3), we take voltage as a reference to investigate. The simulation voltage excitation is 1V sine wave. The radiuses of the coils are 5.5 mm and 11 mm respectively.

The distance between the coil and the transducer  $d$  is 15 mm. The pressure is computed using finite element method [11].

Figure 2 The simulation scheme.

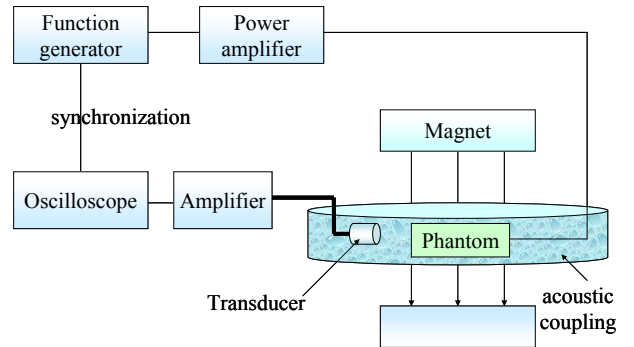


### B. Experiment method

The experiments will also be conducted to study the MAT method, and to validate the simulation results.

The experimental scheme is showed in Fig.3. The function generator and power amplifier generates the voltage excitation with a  $\mu$ s pulses width [12]. The excitation pulse width is 1 $\mu$ s. The load  $R$  is 5.3 Ohm. The imaging object is placed between the two poles of a permanent magnet. The permanent magnet creates a static magnetic field. The static magnetic field  $B$  is 0.45T. The transducer points horizontally to the object. The central frequency of the transducer is 1MHz. For good coupling of acoustic signal, both the transducer and the object are immersed in water. The transducer is scanned around the object in a circular orbit. The oscilloscope is synchronized by function generator while sampling. The signal from the transducer is 1000 times amplified by the amplifier.

Figure 3 Experimental scheme of the magneto-acoustic imaging.

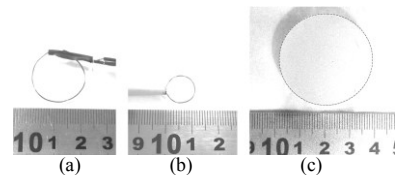


The coil lies horizontally. The radiuses of the coils are 5.5 mm and 11 mm respectively, the distance between the coil and the transducer  $d$  is 15 mm.

Furthermore, an experiment of phantom is also done. The phantom is made of agar with 10% KCl. The radius of the phantom is 17mm.

The imaging object and phantom are showed in Fig. 4.

Figure 4 Photos of the imaging objects. (a) copper coil imaging object with 11 mm radius; (b) copper coil imaging object with 5.5 mm radius (c) agar phantom (10 KCl) with 17mm radius.



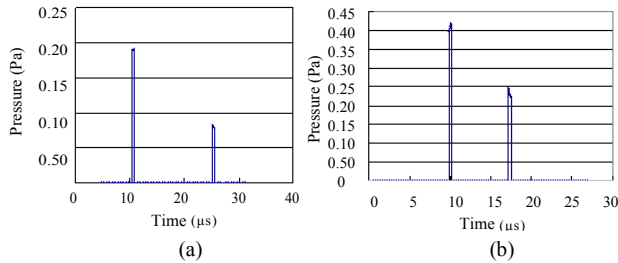
## II. RESULTS

### A. Simulation results

We use 1MHz signal to excite the imaging object. The multi-physics finite element method is used to compute the acoustic pressure using(8). After processing the acoustic field, the signal of the transducer, which locates  $d=15$  mm away from the imaging object (showed as Fig. 2) can be received.

Simulation results are showed in Fig.5. It shows that the acoustic signal can be generated and measured when the imaging objects located in the static magnet field is excited by the current. The time interval of the acoustic pulse response reflects the spatial conductivity edges of the imaging objects.

Figure 5 Simulating results of the coil imaging object. (Test distance  $d=15$  mm). (a)coil radius=11 mm; (b)coil radius=5.5 mm



### B. Experimental results

In the experiments, we set the voltage excitation pulse to 5Vpp, 1Vpp, 0.25 Vpp (peak-to-peak), then the acoustic response signals from the imaging objects (showed in Fig.4) are measured by transducer. The measured signals are showed in Fig.6, Fig.7, and Fig.8.

The electromagnetic pulse marked in the figures is generated by the spatial magnetic field coupling. The velocity of the electromagnetic wave ( $3 \times 10^8$  m/s) is much faster than the acoustic velocity in the water. Therefore, the pulse can be seemed as the initial time.

As Fig.6 shows, the acoustic response reduces as the excitation reduces. When the voltage excitation amplitude is 5V, the acoustic signal is about 10 to 20  $\mu$ V. While the excitation is 0.25 V, it reduces to about 1  $\mu$ V accordingly.

Besides, for the coil with 22 mm diameter, the time interval between the measured signals response is  $\Delta t = \Delta d/v = 22 \times 10^{-3}/1500 = 14.7 \mu$ s, when the acoustic velocity in water is  $v=1500$  m/s. The measured signal is accord with the position in which the conductivity changes.

We notice that there are some small pulses at the right of the two pulses. The reason is, in the experiment the wire is fold to make sure the whole imaging object is fix firmly at the bottom of the water tank. In fact, these pulses can be eliminated when the experimental setup is improved.

Likewise, Fig.7 shows the acoustic signal of  $r=5.5$ mm coil. The voltage excitation is 1V. The spatial distance is 11 mm, while the pulse interval is about  $\Delta t = 7.33 \mu$ s. The time interval is accord with the conductivity location in the special distance. Similarly, the folded wire induces some false pulsed in the right of the two pulses.

Fig. 8 shows the phantom experimental result. We can see pulses reflects the front and back boundary of the

phantom. However, the noise is relative big, so the precision may be improved, to achieve a better signal quality.

Figure 6 Experimental results of the coil with 11mm radius. (The signal is averaged by 512 times; x-axis: time (4  $\mu$ s/div), y-axis: measured voltage; CH 1 is 1/100 of the stimulation, CH2 is measured signal after amplified). (a) the stimulation is 5 V and amplifier gain is 100 (CH1: 20mV/div, CH2: 1mV/div); (b) the stimulation is 1 V and amplifier gain is 1000(CH1: 5mV/div, CH2: 10mV/div); (c) the stimulation is 0.25 V and amplifier gain is 1 000 (CH1: 2mV/div, CH2: 5mV/div)

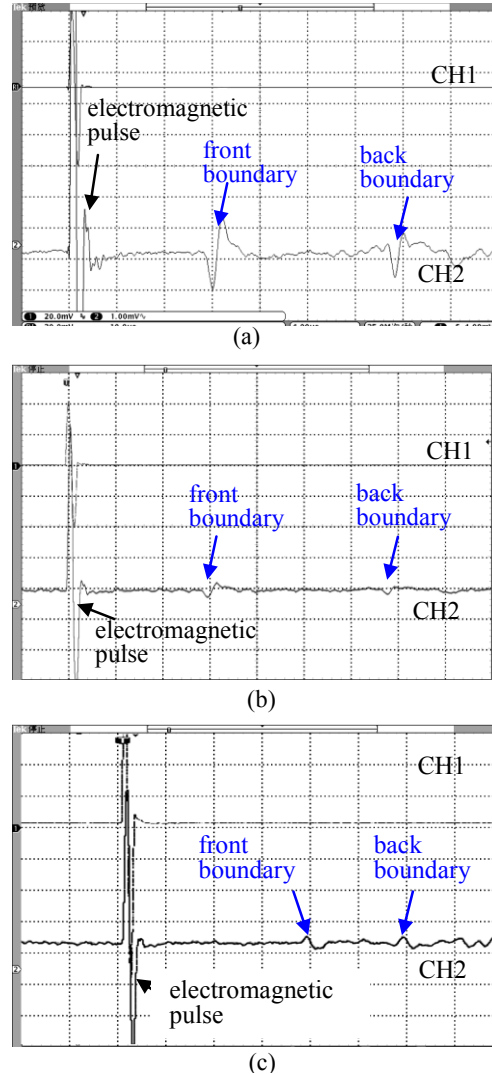


Figure 7 Experimental result of 5.5mm radius coil (The signal is averaged by 512 times; x-axis: time (4  $\mu$ s/div), CH1 is 1/100 of the stimulation (2 mV/div), CH2 is measured voltage signal after amplified (1 mV/div))

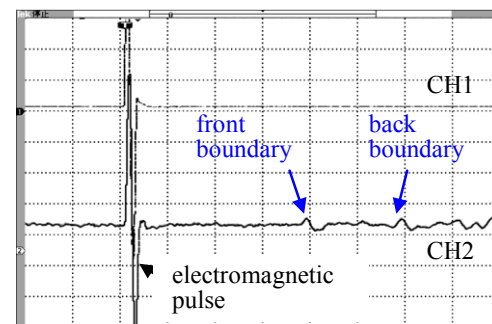
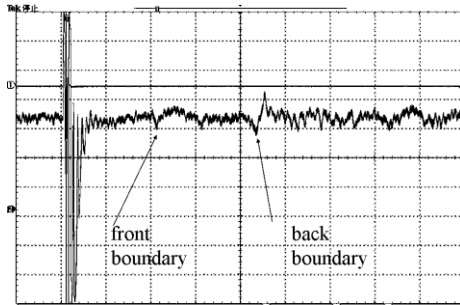


Figure 8 Experimental result of phantom with 17mm radius (The voltage excitation is 34Vpp. The measured signal is averaged by 512 times; x-axis: time (10  $\mu$ s/div), CH1 is 1/100 of the stimulation (50 mV/div), CH2 is the measured signal after amplified (2 mV/div))

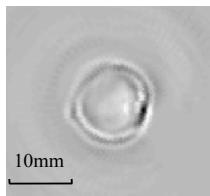


### C. Reconstruction results

We reconstruct the conductivity imaging of the coil imaging object with 5.5 mm radius as Fig.9 shows. The scan step is  $5^\circ$ . The whole scan range is  $300^\circ$ , due to the limit of the experiment setup.

We use back-projection method to reconstruct the conductivity image of the imaging object [13]. The reconstruction result demonstrates that, the imaging reflects the conductivity edge position of the object, where the Lorentz force is big, so it makes a pulse in the corresponding acoustic signal. However, the measured signal is affected by the pulse noise, which made the image has many fake stripes. They can be eliminated by improving the precision of the experimental setup and the reconstruction algorithm.

Figure 9 Reconstruction result of the coil imaging object (radius=5.5 mm)



### III. CONCLUSION AND DISCUSSION

In summary, magneto-acoustic tomography (MAT) approach is a new imaging technique for the high resolution imaging of the electrical impedance distribution. Simulations using the finite element method and the imaging experiments to the coil imaging object and agar phantom have been done in this study. Simulation results showed that the distribution of the acoustic source reflects the sharp change of conductivity produced by the boundary of the objects. Results of the simulation and experiment were in a good agreement, and the resolution of the reconstructed images was less than 1 cm, while the theoretically can reach mm by using the  $\mu$ s pulse excitation. It demonstrates that the feasibility of the MAT approach for bioimpedance imaging to the tissue.

Compared with other imaging method such as MAT-MI, which is reported by He et al [1][9], this method can reduce the requirement to high intensity of current excitation for simple imaging objects study, thus it reduce the cost of the high pulse generator to give the high excitation. However, the weak signal caused by "shielding effect" should be further studied. Besides, several tasks should also be done in the future to lead the technique to clinic application. Firstly, the more complex medium such as excited tissue should be

studied. Secondly, the simple experiment setup limits the precision of the measurement so it should be improved to achieve a better precision. Also, a more accurate study of the influence of instrumentation errors in the image quality is necessary. Besides, the measured signal is weak, which is affected by the noise, so the new method to measure and process the signal could be introduced in the MAT imaging. Other imaging method such as ultrasonic imaging [14] and photo-acoustic imaging [15] may be irradiative.

### ACKNOWLEDGMENT

This research is supported by National Natural Science Foundation of China (81171424) and (51137004)

### REFERENCES

- [1] Xu Yuan, He Bin, "Magnetoacoustic tomography with magnetic induction (MAT-MI)," *Phys. Med. Biol.*, vol. 50, 2005, pp. 5175-5187.
- [2] Gabriel C, Gabriel S, and Corthout E., "The dielectric properties of biological tissues I: Literature survey," *Phys Med Biol*, vol. 41(11) 1996, pp. 2231-2249.
- [3] Gabriel S, Lau RW, and Gabriel C., "The dielectric properties of biological tissues II: Measurements on the frequency range 10Hz to 20GHz," *Phys Med Biol*, vol. 41(11), 1996, pp. 2251-2269.
- [4] Gabriel S, Lau RW, and Gabriel C., "The dielectric properties of biological tissues III: Parametric models for the dielectric spectrum of tissues," *Phys Med Biol*, vol. 41(11), 1996, pp. 2271-2293.
- [5] Fear EC, Hagness SC, Meaney PM, *et al*, "Enhancing breast tumor detection with near-field imaging," *IEEE Microwave Magazine*, vol. 3, 2002, pp. 48-56.
- [6] Bradley J. Roth P, and Basser J, "A theoretical model for magneto-acoustic imaging of bioelectric currents," *IEEE Trans. on Biomedical Engineering*, vol 41, 1994, pp. 723-728.
- [7] Wen H, Shah J, Balaban RS, "Hall effect imaging," *IEEE Trans. on Biomedical Engineering*, vol. 45(1), 1998, pp.119-24.
- [8] Leonid Kunyansky, "A mathematical model and inversion procedure for magneto-acousto-electric tomography," *Inverse Problems*, vol. 28(3), 2012, pp.035002.
- [9] Li Xu, He Bin, "Multi-excitation Magnetoacoustic Tomography With Magnetic Induction for Bioimpedance Imaging," *IEEE Trans. on Medical Imaging*, vol. 29(10), 2010, pp. 1759-1767.
- [10] Zhou Lian, Li Xu, Zhu Shanan, *et al*, "Magnetoacoustic tomography with magnetic induction (MAT-MI) for breast tumor imaging: numerical modeling and simulation," *Phys Med Biol*, vol. 56, 2011, pp. 1967-1983.
- [11] Xu Guo-hui, Liu Zhi-peng, Li Jing-yu, *et al*, "Mathematical model and simulation of forward problem on the magnetoacoustic tomography with magnetic induction," *Chinese Journal of Biomedical Engineering*, vol. 28(4), 2009, pp. 481-484, 489.
- [12] Zhang Shun-qi, Liu Zhi-peng, Jin Jing-na, *et al*, "Design of exciting source for pulsed magnetic field used in MAT-MI System," *Chinese Medical Equipment Journal*, vol. 31(9), 2010, pp. 18-21.
- [13] Ma Hong-xia, Liu Zhi-peng, Zhang Shun-qi, *et al*, "Simulation of acoustic source reconstruction of magnetoacoustic tomography with magnetic induction based on different geometric models," *Chinese Journal of Biomedical Engineering*, vol. 30(1), 2011, pp. 40-45.
- [14] Wan Ming-xi. "Biomedical Ultrasonics," *Science Press*, 2010, pp. 210-344.
- [15] Xu Minghua, Wang Lihong, "Analytic explanation of spatial resolution related to bandwidth and detector aperture size in thermoacoustic or photoacoustic reconstruction," *Physical Review*, E67, 2003, pp. 056605.